DOI: 10.1021/ma901102q

Macromolecules
ARTICLE

# Rouse-Model-Based Description of the Dielectric Relaxation of Nonentangled Linear 1,4-*cis*-Polyisoprene

**Clément Riedel,*[,†,‡,§] Angel Alegría,[§,∥] Philippe Tordjeman,[⊥] and Juan Colmenero[†,§,∥]**

[†]*Donostia Internacional Physics Center, Paseo Manuel de Lardizabal 4, 20018 San Sebastián, Spain,* [‡]*IES - Groupe Micro Rhéo Acoustique - UMR5214, Université Montpellier 2-CC/084, Place Eugène Bataillon, 34095 Montpellier, France,* [§]*Departamento de Física de Materiales UPV/EHU, Apdo. 1072, 20080 San Sebastián, Spain,* [∥]*Centro de Física de Materiales (UPV/EHU-CSIC) - Material Physics Center (MPC), and* [⊥]*Institut de Mécanique des Fluides de Toulouse, Université de Toulouse-CNRS, 1 Allée du Professeur Camille Soula, 31400 Toulouse, France*

*Received May 21, 2009; Revised Manuscript Received September 16, 2009*

ABSTRACT: A detailed test of the Rouse model has been performed on a nonentangled 1,4-*cis*-poly(isoprene) (PI) by investigating the end-to-end vector dynamics by means of broadband dielectric spectroscopy. The contribution to the dielectric relaxation of the end-to-end vector dynamics was determined by subtracting the signal from the local segmental dynamics dominating at higher frequencies. This signal was inferred from experiments on higher molecular weight samples. Our results show that the Rouse model accounts remarkably well for the experimental data once the narrow distribution of molecular masses is properly accounted for. The very same approach is found to provide a good description of a simultaneous dielectric/rheology experiment. Despite the overall good agreement between experiments and model predictions, small excess contributions in the high frequency side of the dielectric losses are detectable.

## Introduction

The chain dynamics of linear polymers is one of the basic and classical problems of polymer physics, and thereby, it has been the subject of intensive investigation, both experimentally and theoretically, over many years.[1−21] Despite of the broad range of models and theoretical approaches existing in the literature, there are many aspects of the problem that remain to be understood (see refs 3 and 10−15 and references therein). Most of the current investigations are devoted to the problem of the dynamics of highly entangled polymer melts with different architectures and topologies and to the rheology of polymer systems of industrial relevance.[11−13] Concerning the chain dynamics of unentangled polymers, it is generally assumed that the well-known Rouse model[10] provides a suitable theoretical description. The Rouse model represents a linear chain as a series of beds and springs subjected to entropic forces in a medium with a constant friction. Although this simple approach obviously fails in describing the melt dynamics of long chains at longer times, the Rouse model is also used for describing the fastest part of the response of these long chains, and thereby it is a common ingredient of all available model and theories. The validity of the Rouse model has been instigated by means of different experimental techniques[2,4,5,9,15,16] and also by molecular dynamics simulations.[17−24] Even so, a full and detailed test of the Rouse model is challenging because in unentangled polymer melts the segmental dynamics (α-relaxation) contributions overlap significantly with the high-frequency components of the chain dynamics. In fact, even by microscopic techniques with spatial resolution as neutron scattering, it is rather difficult to distinguish the border between chain and segmental relaxations.[25] This fact, among others, restricts the use of rheology experiments to test accurately the Rouse model on unentangled polymer chains. It is very hard to obtain rheology data of unentanged polymers in the melt. This is due to the rapid relaxation times of the material and the broad spread of the effect of more local molecular mechanisms that affect the stress relaxation modulus at higher frequencies. Another related limitation of rheological techniques is the rather narrow frequency range usually accessible by such techniques.

More detailed information about chain dynamics of unentangled polymers can be obtained by means of broadband dielectric spectroscopy (BDS) using A-type polymers in the Stockmayer classification.[26] Those polymers contain dipole moments along the chain backbone that do not cancel at the whole chain, giving rise to an "end-to-end" net polarization vector. In addition, they also have dipole moment components perpendicular to the chain contour, as other types of polymers. It is nowadays well-known that the dielectric spectrum of any A-type polymer contains two different relaxation processes. One of them, the segmental relaxation process, is due to fluctuations of the perpendicular dipolar component, whereas the other, the so-called "normal mode relaxation", reflects the fluctuation of the end-to-end vector, $\vec{R}$. The correlation function of this vector $\langle \vec{R}(t)\cdot\vec{R}(0)\rangle$ can be expressed in terms of the discrete Rouse model as

$$\langle \vec{\mathrm{R}}(t)\cdot\vec{\mathrm{R}}(0)\rangle = \frac{2b^2}{N}\sum_{p:\mathrm{odd}}^{N-1}\cot^2\left(\frac{p\pi}{2N}\right)\exp\left(-\frac{t}{\tau_p}\right) \qquad (1)$$

where $N$ is the number of beads and $b$ is the size of the $N-1$ bonds in the chain ($b^2(N-1)$ is the unperturbed chain mean squared end-to-end distance). $\tau_p$ is the relaxation time associated with the Rouse mode $p$ and is given by

$$\tau_p = \frac{\xi b^2}{12k_{\mathrm{B}}T\sin^2(\pi p/2N)} = \frac{\tau_{\mathrm{S}}}{\sin^2(\pi p/2N)} \qquad (2)$$

*Corresponding author: e-mail riedel@ies.univ-montp2.fr.

 Published on Web 10/07/2009 

where $\xi$ is a constant monomeric friction coefficient, $T$ the absolute temperature, $k_B$ Boltzmann's constant, and $\tau_S$ the "segmental" Rouse time ($\tau_S \equiv \tau_{p=N}$). $\tau_S$ is a time which apparently does not have a clear physical meaning (the fastest Rouse time would be $\tau_{p=N-1}$), but it can be related with the so-called characteristic Rouse frequency ($W = 3k_BT/\xi b^2$) as $\tau_S^{-1} = 4W$. Nevertheless, $\tau_S$ is here used as a convenient parameter for the further analysis. Equation 1 shows that only the odd Rouse modes contribute to the end-to-end vector correlation function. Moreover, the contribution from the high $p$ numbers is strongly suppressed due to the amplitude factor, which for low $p$ values approximately behaves as $1/p^2$. Therefore, the end-to-end correlation function, and thereby the dielectric normal mode process, is dominated by the slow (low-$p$) Rouse modes. This is in stark contrast with the stress relaxation where the decay is equally distributed among all modes. This fact facilitates resolving normal mode and segmental relaxation contributions by dielectric spectroscopy. Moreover, the broad frequency range covered by BDS allows accessing simultaneously to both contributions (normal mode and segmental relaxation) at the same temperature. This is a decisive condition for any adequate separation of both relaxations in experimental data. Note that both dynamical processes usually depict distinct temperature dependences,[6,27] which limits the applicability of the time−temperature superposition (TTS) principle in the overlapping range.

One of the canonical A-type polymer is 1,4-*cis*-polyisoprene (PI), which can be obtained by anionic polymerization with a narrow distribution of molecular weights. Dielectric measurements of both the segmental and normal modes of linear PI with different molecular weights (mainly entangled systems) have been reported in the literature many years ago.[4−6,13] From these works, it is well-known that the segmental relaxation of PI has relaxation times essentially independent of the chain molecular weight (provided it is sufficiently large to make the chain-end group effect negligible) whereas the normal mode relaxation time strongly depends on molecular weight. In linear chains, this dependence presents a clear crossover around the entanglement molecular weight of PI (5017 g/mol according to ref 9). For polymers of lower molecular mass, where no entanglements exists, the molecular weight dependence follows, with good approximation, the behavior expected from the Rouse model; i.e., the normal mode relaxation time scales as $M^2$. Thus, in this molecular weight range, it is expected that the normal mode relaxation spectrum, reflecting the fluctuations of the end-to-end vector, could also be well described by the Rouse model. This question has been recently investigated by means of BDS on a rather low molecular weight PI sample ($M_w$ = 1300 g/mol).[15] The authors concluded that the model describe satisfactorily the normal mode relaxation despite the presence of some noticeable deviations at high frequencies. However, the reported experimental data show that the normal mode peak itself is noticeably broader than that predicted by eq 1 (see Figure 7a of ref 15). Nevertheless, the low molecular weight of the sample used for such a test provoked a very pronounced overlapping of the segmental relaxation with the normal mode, which made the detailed comparison difficult. As already mentioned, this is an intrinsic difficulty in testing the Rouse model because for relatively low molecular weight polymer melts the whole chain dynamics occurs in a time/frequency range where non-negligible contributions from the more local segmental dynamics takes place, namely in the high frequency side of the whole chain response.

In this work we have investigated in full detail the accuracy of the Rouse model in describing the normal mode dielectric relaxation. To this end, we have compared the model predictions with the dielectric loss spectrum determined by means of broadband dielectric relaxation experiments in the frequency range $10^{-2}$−$10^6$ Hz on a low polydisperse linear 1,4-*cis*-polyisoprene sample with molecular weight $M_w$ = 2900 g/mol, i.e., well below the molecular weight between entanglements, but high enough to provide a rather good separation between the normal mode and the segmental relaxations. PI samples with different molecular weights in the range $10^3$−$10^5$ g/mol were also investigated. These additional experiments allowed us to model the α-relaxation contribution to the whole relaxation curve and consequently to resolve properly the normal mode response contribution. Our main finding is that the Rouse model can account near perfectly for the experimental dielectric relaxation spectra, but only when the effect of the (small) molecular weight distribution is properly taken into account. This finding has been further tested analyzing in a single framework the data obtained from a simultaneous dielectric and rheology experiment on the same sample. Both rheology and dielectric data are well accounted simultaneously by the Rouse model by using a single parameter set.

**Table 1. Microstructure of the Samples Investigated in This Work[a]**

| sample | $M_n$ [g/mol] | $M_w$ [g/mol] | $I_p$ | $T_g$ (DSC) [K] |
|---|---|---|---|---|
| PI-12 | 1 100 | 1 200 | 1.11 | 194 |
| PI-29 | 2 700 | 2 900 | 1.06 | 203 |
| PI-100 | 10 100 | 10 500 | 1.04 | 209 |
| PI-345 | 33 500 | 34 500 | 1.04 | 210 |
| PI-820 | 76 500 | 82 000 | 1.07 | 210 |

[a] $M_n$ is the average molecular weight, $M_w$ is the weight-averaged molecular weight, $I_p$ is the polydispersivity index, and $T_g$ represents the glass transition temperature determined from the middle point in the DSC heating scan.

## Experimental Section

**Materials.** 1,4-*cis*-Polyisoprene samples were provided by Polymer Source. They were synthesized by living anionic polymerization of isoprene in apolar media. After polymerization, the poly(isoprene) backbone is constituted mainly by *cis* units (80%). The molecular weight ($M_n$) and polydispersity index (determined from size-exclusion chromatography experiments) of the samples investigated are listed in Table 1. To avoid oxidation, PI samples were stored at −25 °C. In addition, before the experiments samples were dried in a vacuum oven at 70 °C for 24 h to remove any trace of solvent.

**Dielectric Spectroscopy.** A broadband dielectric spectrometer, Novocontrol Alpha analyzer, was used to measure the complex dielectric permittivity, $\varepsilon^*(\omega) = \varepsilon'(\omega) - i\varepsilon''(\omega)$, $\omega = 2\pi f$, in the frequency ($f$) range $10^{-1}$−$10^6$ Hz. The samples were placed between parallel gold-plated electrodes of 20 mm diameter. The value of the gap between the electrodes was fixed to 0.1 mm (by a narrow PTFE cross shape piece). The measurements accuracy in the whole frequency range was better than $2 \times 10^{-4}$ for the dielectric loss permittivity. Isothermal measurements were performed every 10 deg over the temperature range 220−300 K using a temperature controller based on $N_2$-gas jet stream (Quatro form Novocontrol). The temperature stability was in all the cases better than ±0.1 K.

**Rheology.** The complex shear modulus $G^*(\omega)$ were measured with a rotational rheometer ARES-LS2 from TA Instruments in the $\omega$ range $10^{-1}$−$4 \times 10^2$ $s^{-1}$. Measurements were performed with two transducers (2K FRTN1 and 200 FRTN1) under a $N_2$ atmosphere, and the temperature was set by the LN2 controller. The samples were placed in between parallel plate tools with a diameter of 8 mm, and a gap of 1.3 mm was used. Using this geometry, it was possible to access not only to the terminal relaxation, precursor of the Newtonian flow, but also to the intermediate region where the segmental dynamics also contributes to the rheological behavior.

Moreover, we also realized an experiment were both dielectric permittivity and shear modulus were measured at the same time in the same setup in order to obtain the very same conditions

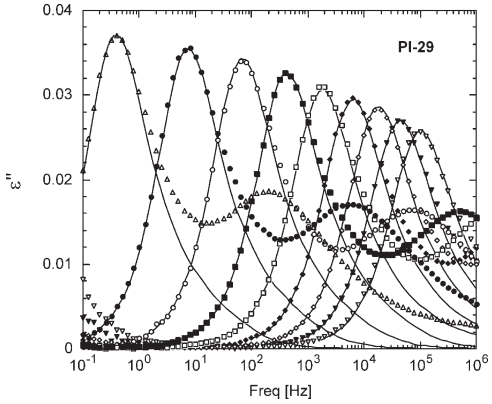


**Figure 1.** Normal mode and α-relaxation of PI-29 at different temperatures. Considering one data set, the normal mode is at low frequency while the α-relaxation appears at higher frequency. The data are measurements from 220 K (left) to 300 K (right) with temperature steps of 10 K. Lines represent the normal mode contribution calculated with the Rouse model taking the actual sample polydispersity into account (see text).

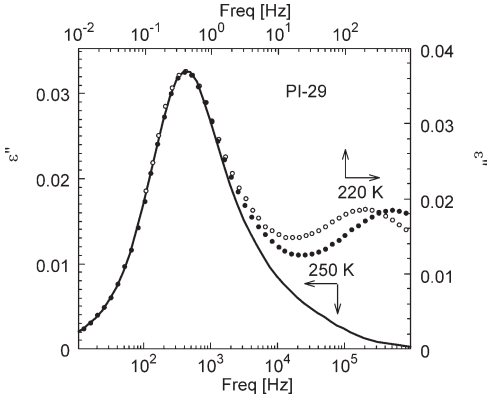


**Figure 2.** Comparison of normal mode and α-relaxation frequency shifts for PI-29 when temperature is changed from 220 to 250 K. The curve at 220 K has been shifted and scaled to match the normal mode peak at 250 K. The clear failure in overlapping for the α-relaxation can be observed at higher frequency. Line represents the normal mode contribution calculated with the Rouse model taking the actual sample polydispersity into account (see text).

(sample, temperature, ...). The sample was placed between the dielectric tools of the rheometer consisting of two parallel plates (25 mm diameter) electrically isolated from the rheometer body. Thus, the rheology experiment was performed with the ARES-LS2 while an electric impedance analyzer from Novocontrol realized the dielectric experiment. No interference between both experiments was detected. Although in these experiments the sample thickness (0.9 mm) was relatively large for an optimum dielectric test with high accuracy, but relatively small for a convenient rheology experiment, the simultaneous experiment removes any effect of using different sample geometry/preparation and different temperature reading; the latter could produce spurious frequency shift. These requirements are critical for the detailed test of the Rouse model presented here.

**Differential Scanning Calorimetry.** The glass transition temperatures ($T_g$) of all the compounds were determined by differential scanning calorimetry (DSC) (Q2000 TA Instrument) using 5 mg PI samples, in hermetic Al pans, cooled, and subsequently heated at a common rate of 10 K/min. The glass transition temperature was determined from the middle point of the heat flow step during the heating run. The values obtained for all the PI samples investigated are summarized in Table 1. A significant variation of the obtained value with the molecular weight is found (namely for low molecular masses) in good agreement with literature results.[5]

## Results

**A. Broadband Dielectric Spectroscopy.** Figure 1 shows the high level of accuracy obtained by means of the present BDS experiments when measuring the rather weak dielectric relaxation of a PI-29 sample, for both the normal mode and the α-relaxation. From simple inspection of the data it is apparent that the normal mode peak shifts by changing temperature without any significant change in shape (time−temperature superposition is verified for this process), which is one of the predictions of the Rouse model (see eq 1). However, it is also evident that the shift of the normal mode peak is distinct than that of the α-relaxation one; i.e., the TTS fails for the complete response.[6,27] This fact is illustrated in Figure 2 where data at two temperatures where both processes are clearly visible in the frequency window are compared. For this comparison the axes were scaled (by a multiplying factor) in such a way that the normal peaks superimpose. Whereas the superposition in the normal mode range is excellent, the same shift makes the α-relaxation peak

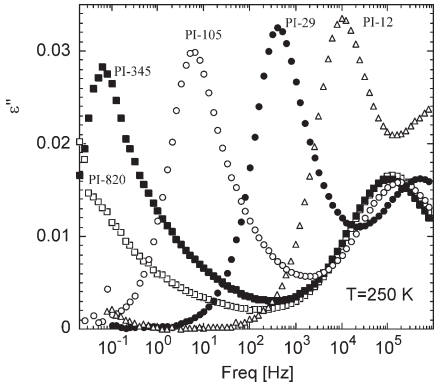


**Figure 3.** Dielectric relaxation curves collected at 250 K on 1,4-*cis*-polyisoprene with different molecular weights.

positions to be about half a decade different. In Figure 3 the data recorded at a common temperature for samples with varying molecular weight are presented. It is remarkable that not only the normal mode changes in position with molecular weight but also the α-relaxation peak. The latter is consistent with the previously reported results.[5] When considering the temperature dependence of the normal mode peak (temperature dependence of the shift factor) we found that, whereas for high molecular masses (above that between entanglements) they are the same within uncertainties (Williams−Landel−Ferry equation parameters with $T_g$ as the reference temperature $C_1 = 30.2 \pm 0.7$ and $C_2 = 57.0 \pm 0.2$ K), for lower molecular weight samples the value of $C_1$ remains the same but $C_2$ becomes noticeably smaller, being 49.2 K for PI-29. This is likely related with the significant variation of $T_g$ in the low molecular range (see Table 1).

**B. Rheology.** The data resulting from the rheology experiments performed on a PI-29 sample of 1.3 mm thickness using two parallel plates of 8 mm diameter are shown in Figure 4a. To produce this plot a master curve at a reference temperature $T_r = 230$ K was built imposing the horizontal shift factor $a_T$ determined from BDS (see above) and a vertical shift factor $b_T = T_r/T$. It is apparent that the superposition so obtained is good in the terminal relaxation range, although at the highest frequencies, where the contributions of the segmental dynamics are prominent, the data superposition fails clearly. The use of master curves in rheology

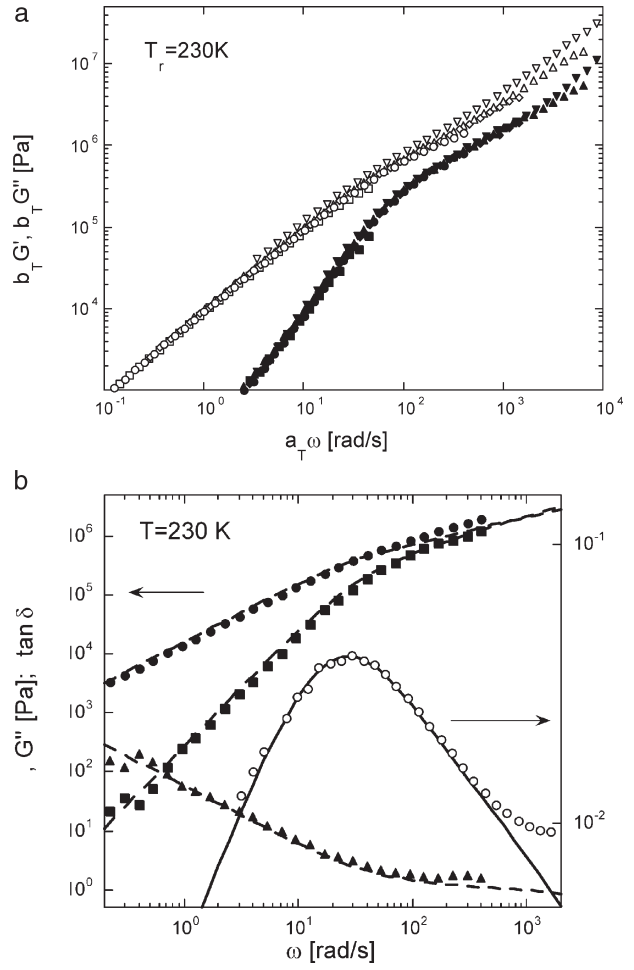


**Figure 4.** (a) Master plot (reference temperature $T_r = 230$ K) of the real and imaginary parts of the shear modulus, $G^*(\omega)$ ($G'$, filled symbols; $G''$, empty symbols) from PI-29, measured at different temperatures (215 K, inverted triangles; 220 K, triangles; 225 K, diamonds; 230 K, circles; and 240 K, squares). Data have been shifted horizontally by using the shift factors derived from the BDS experiments and a vertical scaling $b_T = T_r/T$ was also applied. (b) Simultaneous rheology ($G'$, filled squares; $G''$, filled circles; tan $\delta$, filled triangles) and BDS experiments ($\varepsilon''$, empty circles) on PI-29 at 230 K. Lines correspond to the description obtained using the Rouse model, with a single set of parameters, for all the data sets.

experiments is a standard practice because of the rather limited frequency range and the general applicability of the TTS principle to the terminal relaxation range. However, the presence of the segmental dynamics contribution at high frequencies when approaching $T_g$ could make the application of TTS questionable because the different temperature shifts of global and the segmental dynamics (see above). Thus, using rheology data alone, the high frequency side of the terminal region could be highly distorted.

In addition, simultaneous dielectric and rheology experiments on the same piece of a PI-29 sample were also conducted at a selected temperature of 230 K. In this case the sample thickness was smaller to balance the data quality of both dielectric and rheological results. We found that a thickness of 0.9 mm provides a rather good compromise. The output of these experiments at 230 K is shown in Figure 4b. Despite the very different geometry used, the rheological results are in close agreement with those obtained before. In this simultaneous experiment, the dielectric normal mode is clearly resolved so the peak position defining the time scale can be determined with low uncertainty, although again the

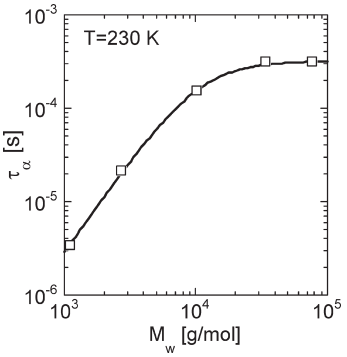


**Figure 5.** α-Relaxation times of polyisoprene at 230 K as a function of molecular weight. The line corresponds to eq 5.

accuracy of the dielectric relaxation data is not so good as that obtained in the data presented before. Nevertheless, this experiment will be essential in testing the ability of the Rouse model in accounting simultaneously for both the dielectric and rheology signatures of the whole chain dynamics.

**C. Data Analysis.** *Dielectric* α*-Relaxation.* In order to describe the segmental relaxation of the PI samples, which overlaps with the normal mode (NM) at the higher frequencies, the imaginary part of the obtained dielectric permittivity in this range was analyzed by using the phenomenological Havriliak−Negami (HN) function[28,29]

$$\varepsilon^*(\omega) = \varepsilon_\infty + \frac{\Delta\varepsilon}{[1 + (i\omega\tau_{HN})^\beta]^\gamma} \tag{3}$$

where $\Delta\varepsilon = \varepsilon_s - \varepsilon_\infty$, $\varepsilon_\infty$ and $\varepsilon_s$ are the unrelaxed and relaxed values of the dielectric constant, and $\tau_{HN}$ is a characteristic relaxation time. In addition, a power law contribution ($\propto \omega^{-1}$) was used to account for the normal mode contribution at low frequencies, which is the frequency dependence expected from the Rouse model for frequencies larger than the characteristic one of the shortest mode contribution. Thus, we assumed that the high frequency tail of the normal mode follows a $C/\omega$ law and superimposes on the low frequency part of the α-relaxation losses, $C$ being a free fitting parameter at this stage. In eq 3, $\beta$ and $\gamma$ are shape parameters ($0 < \beta, \gamma \leq 1$) describing respectively the symmetric and the asymmetric broadening of the equivalent relaxation time distribution function. The α-relaxation time corresponding to the loss peak maximum was obtained from the parameters of the HN function as follows:[29]

$$\tau_\alpha = \tau_{HN} \frac{\left[\sin\left(\frac{\beta\gamma\pi}{2+2\gamma}\right)\right]^{1/\beta}}{\left[\sin\left(\frac{\beta\pi}{2+2\gamma}\right)\right]^{1/\beta}} \tag{4}$$

The results obtained for samples with different molecular weight at a common temperature of 230 K are shown in Figure 5. It is evident that in the low molecular weight range the time scale of the segmental dynamics is considerably faster than that corresponding to the high molecular weight limit. This behavior is mainly associated with the plasticizer like effect of the end-chain groups, which are more and more relevant as chain molecular weight decreases. The line in Figure 5 describing the experimental behavior for the PI samples investigated is given by

$$\tau_\alpha(M) = \frac{\tau_\alpha(\infty)}{1 + (10000/M)^2} \tag{5}$$

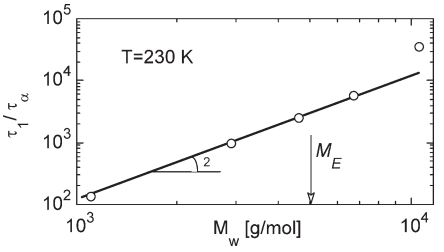


**Figure 6.** Ratio $\tau_1/\tau_\alpha$ as a function of the molecular weight at 230 K. Solid line represents the behavior predicted by the Rouse model. The arrow indicates the reported value of $M_E$ for PI.[9]

As observed, the value corresponding to the ideal infinity long chain, $\tau_\alpha(\infty)$, is obtained already for molecular masses above 30 000 g/mol. This is in good agreement with the molecular weight for which the value of $T_g$ no longer depends significantly on molecular weight (see Table 1).

*Dielectric Normal Mode.* As already commented in the Introduction, the dielectric normal mode reflects the fluctuations of the end-to-end vector and is dominated by the slowest chain normal mode. As a consequence, the peak frequency provides a rather direct access to the longest time of eq 2, $\tau_1$, usually called Rouse time. Using these values of $\tau_1$ at 230 K, we have checked whether below the molecular weight between entanglements the Rouse model predictions concerning the molecular weight dependence of the slowest relaxation times is verified. In Figure 6 we present the values of the ratio $\tau_1/\tau_\alpha$ as a function of the molecular mass. The ratio between the longest relaxation time and the value of $\tau_\alpha$ obtained at the same temperature in the same experiment is the way used trying to remove the possible variation in $\tau_1$ arising from the monomeric friction coefficient, which can be assumed as straightforwardly related with the changes in the glass transition temperature and, hence, with the noticeable effect of end-chain groups in the segmental dynamics. In addition to the data of the polymers here investigated, data from other two PI samples previously measured in our laboratory are also included for completeness, namely for PI samples with values of $M_w$ = 6700 g/mol and $M_w$ = 4600 g/mol. Figure 6 shows that below a molecular weight of around 7000 g/mol the data scales approximately with $M^2$. This is just the Rouse model prediction, i.e., what is deduced from eq 2 for low-$p$ values where the following approximation holds:

$$\tau_1 \cong \frac{\xi b^2 N^2}{3k_B T \pi^2} \tag{6}$$

*Rouse-Model-Based Description of the Normal Mode Dielectric Relaxation.* Once we have confirmed the range of molecular masses where the molecular weight dependence of the longest relaxation time verifies eq 6, we will test if the whole dielectric normal mode conforms the Rouse model predictions. We have selected the sample PI-29 for this test because, on the one hand, it has a molecular weight sufficiently below of the molecular weight between entanglements (so all the molecular masses of the distribution are below $M_E$) and, on the other hand, it shows a normal mode that is rather well resolved from the segmental α-relaxation contributions to the dielectric losses (see Figures 1 and 2). Using higher molecular weight samples yield the possibility that the high molecular weight tail of the distribution was above the entanglement molecular weight. On the contrary, for lower molecular weight samples the stronger superposition of the normal mode and the α-relaxation will make the comparison less conclusive. For the test, we have taken the data recorded at a temperature of 230 K where the normal mode contribution is completely included within the experimental frequency window, being at the same time the α-relaxation contribution also well captured (see Figure 7).

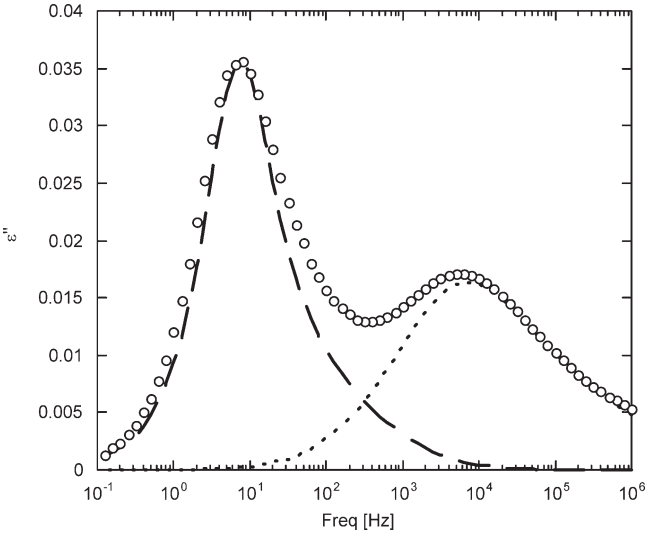


**Figure 7.** Rouse model prediction without taking sample polydispersity into account (dashed line) compared to BDS data points. The dotted line represents the modeled contribution of the α-relaxation (see text).

In order to check if the dielectric normal mode response can be accurately described by the Rouse approach, we have calculated the dielectric loss corresponding to the end-to-end vector correlation function (eq 1). As it has been aforementioned, due to the $1/p^2$ factor, the correlation function is dominated by the low-$p$ Rouse modes. In this framework, the imaginary part of the dielectric permittivity associated with the normal mode results as

$$\varepsilon''(\omega) \propto \frac{2b^2}{N} \sum_{p:\text{odd}}^{N-1} \cot^2\left(\frac{p\pi}{2N}\right) \frac{\omega\tau_p}{1+\omega^2\tau_p{}^2} \tag{7}$$

For using eq 7, we need the previous determination of $N$, which is not known a priori, as it requires the estimation of the bead size. Adachi and co-workers[30] estimated the bead size of PI on the basis of an analysis of the segmental relaxation in terms of a distribution of Debye relaxation times. These authors suggested that a PI bead would contain about seven monomers. However, a generally accepted approach is to consider that the bead size would be of the order of the Kuhn length, $b_K$.[31] The literature value of $b_K$ for PI is 0.84 nm,[32] which corresponds to a molecular mass of the Kuhn segment of 120 g/mol. This means that a Kuhn segment would contain about 1.5 monomers, about a factor of about 5 less than Adachi et al. estimated.

On the other hand, recent results have evidenced that the α-relaxation in the glass transition range probes the polymer segmental motions in a volume comparable to $b_K{}^3$.[33,34] Thus, we can identify the "segmental" Rouse time $\tau_S$ at $T_g$ with the α-relaxation time determined at this same temperature, i.e., $\tau_S(T_g)$ = 5 s. In this way, by using the WLF equation describing the temperature dependence of the normal mode peak, the obtained value of $\tau_S$ at 230 K would be $1.1 \times 10^{-4}$ s. Using this value and that obtained for $\tau_1$ from the normal peak maximum in eq 2, a value of $N$ = 24 results. Note that according to this value the bead mass would be around 121 g/mol, in very good agreement with literature results for the

Kuhn segment mass,[32] and consequently the corresponding bead size will nearly identical to $b_k$.

Thus, in order to test the validity of the Rouse model in describing the dielectric normal mode relaxation data we assumed $N = 24$ in eq 7, which would be completely predictive, except in an amplitude factor, once the slowest relaxation time $\tau_1$ was determined from the loss peak maximum (see above). The so calculated curve is shown as a dashed line in Figure 7. It is very clear that the calculated curve is significantly narrower than the experimental data, not only at high frequencies where some overlapping contribution from the α-relaxation exists, but more importantly also in the low frequency flank of the loss peak. This comparison evidence clearly that the experimental peak is distinctly broader than the calculation of the Rouse model based in eq 7, confirming what was already envisaged in Figure 7a of ref 15. Nevertheless, an obvious reason for this discrepancy could be the fact that the actual sample has some (small) polydispersity. Despite the fact that PI samples with a low polydispersity (Table 1) were chosen, even samples obtained from a very controlled chemistry contains a narrow distribution of the molecular weights, which was not considered in the previous calculation. Moreover, due to the overlapping of the α-relaxation contribution on the high frequency side of the normal mode, a convenient modeling of the faster process is mandatory for a full detailed quantitative checking of the Rouse model predictions. This more elaborated checking is presented below where we first model the contribution to the dielectric response of the more local segmental dynamics in order to completely resolve the normal mode contribution. Moreover, for modeling both the normal mode and the α-relaxation, we need to consider the effects of the actual molecular weight distribution of the sample. Namely, we have assumed a Gaussian-like distribution shape in a first approximation, being therefore the distribution of molecular masses $g(M)$ given by

$$g(M) = \frac{1}{\sqrt{2\pi}\sigma}\exp\left[-\frac{(M-M_n)^2}{2\sigma^2}\right] \text{ with}$$
$$\sigma = M_n\sqrt{\frac{M_w}{M_n}-1} \tag{8}$$

where the values of $M_n$ and $M_w$ are taken from Table 1, hence characterizing the actual sample properties.

As already mentioned, the overlapping the α-relaxation contribution with the whole chain dynamics is an intrinsic problem in checking the Rouse model, since its applicability is limited to chains with moderate molecular weight (below the molecular weight between entanglements). Because the time scale separation between the two dynamical processes is not complete, a detailed analysis of the validity of the Rouse model predictions at high frequencies requires accounting accurately for the α-relaxation contribution. As can be seen in Figure 3, the α-relaxation contribution from long chains is nearly independent of molecular mass, but for low molecular masses (ca. below 20 000 g/mol) it is shifted to higher frequencies and slightly broader (see Figure 5). Because the rather small length scale involved in the segmental dynamics (around a nanometer),[31,33] it is expected that for a relatively low molecular weight sample, as PI-29, there would be contributions to the α-relaxation with different time scales originated because the presence of chains of different lengths. This could explain the fact that the α-relaxation peak of the PI-29 sample is slightly broader than that of a high molecular weight one, the PI-820 for instance (see Figure 3). Thus, in order to take this small effect into account, we decided to describe the α-relaxation of the PI-29 sample as a superposition of different contributions. The contribution to the α-relaxation from a single chain of molecular weight $M$ is assumed to be of the HN type (eq 3), with intensity $\Delta\varepsilon(M)$ proportional to the number of units (segments) in the chain, i.e., proportional to $M$. Under this assumption, the whole α-relaxation would be given as follows:

$$\varepsilon^*_\alpha(\omega) = \int \frac{\Delta\varepsilon(M)}{[1+(i\omega\tau_{HN}(M))^\beta]^\gamma} g(M)\,dM$$
$$= \frac{\Delta\varepsilon_\alpha}{M_n}\int \frac{M}{[1+(i\omega\tau_{HN}(M))^\beta]^\gamma} g(M)\,dM \tag{9}$$

where $g(M)\,dM$ is the number density of chains with molecular weight $M$, $\Delta\varepsilon_\alpha$ is the total dielectric strength associated with the α-relaxation, and $1/M_n$ is just the normalization factor. The parameters $\beta$ and $\gamma$ in eq 9 were taken form the fitting of the α-relaxation losses of the highest molecular weight sample PI-820 ($\beta = 0.71$, $\gamma = 0.50$); i.e., the shape of each component has been assumed to be that obtained from the experiment in a sample with a high molecular weight and a narrow distribution. For such a sample no differences between the contributions of distinct chains are expected (see Figure 5). Furthermore, note that for this sample the α-relaxation is very well resolved from the normal mode, and therefore, its shape can be accurately characterized. Moreover, according to eq 5, the following expression for $\tau_{HN}(M)$ was used, $\tau_{HN}(M)/\tau_{HN}(\infty) = [1+(10000/M)^2]^{-1}$, where a value of $\tau_{HN}(\infty) = \tau_{HN}(82000)$ is a good approximation. In order to avoid the unphysical asymptotic behavior ($\varepsilon'' \propto \omega^\beta$) given by the HN equation at very low frequencies, the physical asymptotic behavior ($\varepsilon'' \propto \omega$) was imposed for frequencies 2 decades lower than that of the peak loss frequency. This cutoff frequency was chosen because is the highest cutoff frequency, allowing a good description of the α-relaxation data from the high molecular weight PI samples. The resulting curve is depicted in Figure 7 as a dotted line. The value of $\Delta\varepsilon_\alpha$ (single adjustable parameter) has been selected to fit the experimental data above $f = 5\times10^4$ Hz, where no appreciable contributions from the normal mode would be expected (see dashed line in Figure 7 as a first estimate). After calculating the α-relaxation contribution, the normal mode contribution can be completely resolved by subtracting it from the experimental data. The so-obtained results are depicted in Figure 8 using a log−log representation.

Now, we are in a situation where it becomes possible to perform a detailed comparison between the experimental normal mode relaxation and the calculated Rouse model expectation. In order to incorporate the small sample polydispersity, the response expected from the Rouse model has been calculated as a weighted superposition of the responses corresponding to chains with different molecular weights. Since the molecular masses of the chains in the PI-29 sample are all below the molecular weight between entanglements, the molecular weight dependence of $\tau_p$ will be that given by eq 2 for all of the different chains. For calculating $\tau_p(M)$, we have used in eq 2 a common value $\tau_S$ irrespective of the molecular weight of the particular chain. Furthermore, we calculated $\tau_1(M_w)$ as the reciprocal of the peak angular frequency of the experimental normal mode of this sample. In this way the Rouse model remains completely predictive, and the corresponding dielectric response to be compared

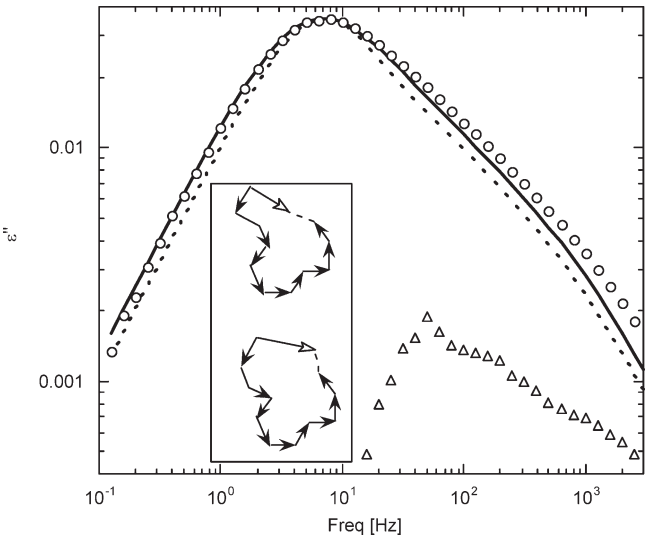


**Figure 8.** Resolved normal mode relaxation of PI-29 sample (see text). The lines represent the behavior predicted by the Rouse model including for the actual sample polydispersity (solid line) and without it (dotted line). Triangles correspond to the difference between the experimental losses and the Rouse model predictions. The inset shows schematically how the presence of configuration defects allows fluctuations of the whole chain dipole moment without variation of the end-to-end vector.

with normal mode contribution from the actual sample will be given by

$$\varepsilon''_N(\omega) = \frac{\Delta\varepsilon_N}{M_n}\int M\frac{2b^2}{N}\sum_{p:\mathrm{odd}}^{N-1}\cot^2\left(\frac{p\pi}{2N}\right)\frac{\omega\tau_p(M)}{1+\omega^2\tau_p(M)^2}g(M)\,\mathrm{d}M \tag{10}$$

where the contribution to the normal mode from a given chain is proportional to the chain dipole moment (to the end-to-end vector) and thus again proportional to $M$. As can be seen in Figure 8 (solid line), this calculation provides a very satisfactory description of the experimental dielectric losses, namely at frequencies around and above the peak. The excellent agreement evidence that taking into account the (small) polydispersity of the sample under investigation is necessary to provide a good description of the dielectric normal mode contribution by means of the Rouse model, without any adjustable parameter other than the Rouse time, which (for the average molecular mass) is essentially determined from the reciprocal of the maximum loss angular frequency. In Figures 1 and 2 we have also included the corresponding Rouse model predictions for the normal mode relaxation to illustrate how it works at all the temperatures investigated.

Despite the overall good agreement, Figure 8 evidences that the experimental losses are slightly larger (maximum difference about 10%) than the Rouse model prediction in the high frequency side. Although one could consider that this is simply due to the contribution of the overlapping α-relaxation that has not been properly subtracted, the fact that the maximum of these extra losses intensity occurs at frequencies 2 decades above the segmental relaxation peak (see triangle in Figure 8) seems to point out to other origin. In agreement with this idea, it is clear in Figure 2 that the frequency distance above the NM peak where the Rouse model description starts underestimating the experimental losses does not depend much on temperature. Thus, extra contributions from some chain modes are detected in the dielectric normal mode. In fact, the peak intensity of the extra losses occurs at the position of the $p = 3$ mode (see triangles in Figure 8), i.e., the second mode contributing to the dielectric normal mode. All this might evidence the fact that the Rouse model approach ignores several aspects of the actual chain properties as that of the chain stiffness[21] or the lower friction expected to occur at the chain ends.[35] In this context it is noticeable that the contribution from the α-relaxation extended considerably toward the frequency range where the normal mode is more prominent. In fact, the cutoff frequency used for describing the α-relaxation in Figure 7 was close to 100 Hz, i.e., where the differences between the normal mode response and the Rouse model are more pronounced. This result indicates that for most of the high-$p$ chain modes the segmental relaxation is not completed. This is in contrast to the assumptions of the Rouse model where it is considered that all the internal motions in the chain segment are so fast that their effect can be included in the effective friction coefficient. It is noteworthy that a higher frequency cutoff would be not compatible with the experimental data of the high molecular weight PI samples and would produce a more prominent underestimation of the dielectric normal mode losses. On the contrary, a lower frequency cutoff would improve slightly the agreement between the normal mode data and the Rouse model prediction but would imply and higher coupling between the segmental dynamics and the whole chain motion.

Small deviations from the Rouse model predictions have also been reported from numerical simulations and molecular dynamics calculations and detected by neutron scattering experiments,[15,21,36,37] although these deviations become evident only for relatively high-$p$ values. Note that dielectric experiments being mainly sensitive to the low-$p$ modes can hardly detect such deviations. On the other hand, experiments in solution have also evidenced differences between the experimental data and the predictions of the Rouse model,[38] which were tentatively attributed to chain overlapping effects since the deviations occur above a given concentration. Nonetheless, there are also possible experimental sources for the small extra high frequency contributions to the dielectric losses as it would be the presence in the actual polymer of a fraction of monomeric units others than the 1,4-*cis* ones (up to 20%). The motion of such units, having a much smaller component of the dipole moment parallel to the chain contour, would produce small amplitude fluctuations of the whole dipole moment uncorrelated with the fluctuations of the end-to-end vector (see inset in Figure 8). The chain motions around these "configuration defects" would generate a relatively weak and fast contribution to the dielectric normal mode that could explain the experimental data. Unfortunately, the actual sample microstructure prevents to definitively address whether the deviations from the Rouse model predictions are actually indicative of its limitations.

**D. Broadband Dielectric Spectroscopy and Rheology in the Same Experiment.** Once we have found that the Rouse model can account accurately for the chain dynamics as observed by dielectric spectroscopy, the question that arise is if using the very same approach it would be possible to account also for other independent experiments, namely rheology. A key point to perform such a test is to be sure that all the environmental sample conditions remains the same. To be sure about this, as already presented, we performed simultaneous dielectric and rheology experiments at 230 K (see Experimental Section), and the resulting experimental data were used to test the accuracy of the Rouse model in describing both set simultaneously. The approach used was to determine $\tau_1$ from the dielectric losses, according with the description used above that is able to accurately account for

the complete dielectric relaxation spectrum, and to use a similar approach to generate the corresponding rheology behavior. Thus, the only unknown parameter needed to perform the comparison with the experimental $G'(\omega)$ and $G''(\omega)$ data will be $G_\infty$ (the high frequency limit of the modulus in terminal zone), which in fact it is not needed for calculating $\tan \delta(\omega) = G''(\omega)/G'(\omega)$. The equations used were

$$G'(\omega) = \frac{G_\infty}{M_n} \int M \sum_p^{N-1} \frac{\omega^2 \tau_p(M)^2/4}{1 + \omega^2 \tau_p(M)^2/4} g(M)\, dM \quad (11a)$$

$$G''(\omega) = \frac{G_\infty}{M_n} \int M \sum_p^{N-1} \frac{\omega \tau_p(M)/2}{1 + \omega^2 \tau_p(M)^2/4} g(M)\, dM \quad (11b)$$

When comparing these equations with the dielectric case, the factor $(\sim 1/p^2)$ appearing in eqs 1 and 7 does not appear in the modulus equations, showing that the contribution of all the modes is equally relevant for the melt rheology. Furthermore, not only odd but also even modes contribute to shear modulus.

The results of the comparison between the calculated responses and the experimental data are shown in Figure 4b. A satisfactory description is obtained for $G'(\omega)$ and $G''(\omega)$ by means of the same Rouse model parameters used in describing the dielectric normal mode. More interestingly, the description of $\tan \delta$ is also rather good, for which the previous calculation is compared with the experimental data without any arbitrary scaling. Despite the good agreement obtained, it is worthy of remark that the ability of rheology experiments for checking the Rouse model in full detail is much more limited than the dielectric one because both the narrower frequency range accessible and the stronger overlapping of the segmental dynamics contributions (see Figure 4).

## Conclusions

By means of broadband dielectric spectroscopy, we have resolved the normal mode relaxation of a nonentangled 1,4-*cis*-polyisoprene (PI) and therefore accessed to the end-to-end vector dynamics over a broad frequency/time range. A remarkably good comparison of the data with the Rouse model predictions is found if the effect of the actual narrow distribution of molecular masses of the sample investigated is accounted. The very same approach was found to provide a good description of a simultaneous dielectric/rheology experiment. The small excess contributions found in the high frequency side of the experimental dielectric NM losses could be associated, at least partially, to the sample microstructure details. Therefore, we conclude that the Rouse model accounts within experimental uncertainties for the end-to-end dynamics of unentangled PI, once the molecular weight distribution effects are considered. A more sensitive test would require an unentangled nearly monodisperse full 1,4-*cis*-polyisoprene sample, which can hardly be available.

**Acknowledgment.** The Donostia International Physics Center (DIPC) financial support is acknowledged. A.A. and J.C. acknowledge the financial support provided by the Basque Country Government (Ref. No. IT-436-07, Depto. Educación, Universidades e Investigación), the Spanish Ministry of Science and Innovation (Grant No. MAT 2007-63681), and the European Community (SOFTCOMP program).

## References and Notes

(1) Ferry, J. D. *Viscoelastic Properties of Polymers*, 3rd ed.; John Wiley & Sons: New York, 1980.
(2) Plazek, D. J. *J. Phys. Chem.* **1965**, *69*, 3480. Plazek, D. J.; O'Rourke, V. M. *J. Polym. Sci., Part A-2* **1971**, *9*, 209.
(3) McLeish, T. C. B. *Adv. Phys.* **2002**, *51*, 1379.
(4) Adachi, K.; Kotaka, T. *Macromolecules* **1985**, *18*, 466. *Macromolecules* **1987**, *20*, 2018. *Prog. Polym. Sci.* **1993**, *3*, 585.
(5) Boese, D.; Kremer, F. *Macromolecules* **1990**, *23*, 829.
(6) Schonhals, A. *Macromolecules* **1993**, *26*, 1309.
(7) Santangelo, P. G.; Roland, C. M. *Macromolecules* **1998**, *31*, 3715.
(8) Abdel-Goad, M.; Pyckhout-Hintzen, W.; Kahle, S.; Allgaier, J.; Richter, D.; Fetters, L. J. *Macromolecules* **2004**, *37*, 8135.
(9) Fetters, L. J.; Lohse, D. J.; Richter, D.; Witten, T. A.; Zirkel, A. *Macromolecules* **1994**, *27*, 4639.
(10) Rouse, P. E., Jr. *J. Chem. Phys.* **1953**, *21*, 1272.
(11) Doi, M.; Edwards, S. F. *The Theory of Polymer Dynamics*; Clarendon: Oxford, 1986.
(12) Likhtman, A. E.; McLeish, T. C. B. *Macromolecules* **2002**, *35*, 6332.
(13) Watanabe, H.; Sawada, T.; Matsumiya, Y. *Macromolecules* **2006**, *39*, 2553.
(14) Kaznessis, Y. N.; Hill, D. A.; Maginna, E. J. *J. Chem. Phys.* **1999**, *111*, 1325.
(15) Doxastakis, M.; Theodorou, D. N.; Fytas, G.; Kremer, F.; Faller, R.; Müller-Plathe, F.; Hadjichristidis, N. *J. Chem. Phys.* **2003**, *119*, 6883.
(16) Richter, D.; Monkenbusch, M.; Arbe, A.; Colmenero, J. *Neutron Spin Echo in Polymer Systems*; Springer-Verlag: Berlin, 2005.
(17) Kremer, K.; Grest, G. S. *J. Chem. Phys.* **1990**, *92*, 5057.
(18) Bennemann, C.; Baschnagel, J.; Paul, W.; Binder, K. *Comput. Theor. Polym. Sci.* **1999**, *9*, 217.
(19) Paul, W.; Smith, G. D. *Rep. Prog. Phys.* **2004**, *67*, 1117.
(20) Moreno, A. J.; Colmenero, J. *Phys. Rev. Lett.* **2008**, *100*, 126001.
(21) Brodeck, M.; Alvarez, F.; Arbe, A.; Juranyi, F.; Unruh, T.; Holderer, O.; Colmenero, J.; Richter, D. *J. Chem. Phys.* **2009**, *130*, 094908.
(22) Ries, M. E.; Klein, P. G.; Brereton, M. G.; Ward, I. M. *Macromolecules* **1998**, *31*, 4950.
(23) Qiu, X.; Ediger, M. D. *Macromolecules* **2000**, *33*, 490.
(24) Paul, W.; Smith, G. D.; Yoon, D. Y.; Farago, B.; Rathgeber, S.; Zirkel, A.; Willner, L.; Richter, D. *Phys. Rev. Lett.* **1998**, *80*, 2346.
(25) Richter, D.; Monkenbusch, M.; Willner, L.; Arbe, A.; Colmenero, J.; Farago, B. *Europhys. Lett.* **2004**, *66*, 239.
(26) Stockmayer, W. H. *Pure Appl. Chem.* **1967**, *15*, 539.
(27) Ding, Y.; Sokolov, A. P. *Macromolecules* **2006**, *39*, 3322.
(28) Havriliak, S.; Negami, S. *Polymer* **1967**, *8*, 161.
(29) Kremer, F.; Schonhals, A. *Broadband Dielectric Spectroscopy*; Springer: Berlin, 2003.
(30) Adachi, K.; Yoshida, H.; Fukui, F.; Kotaka, T. *Macromolecules* **1990**, *23*, 3138.
(31) Inoue, T.; Uematsu, T.; Osaki, K. *Macromolecules* **2002**, *35*, 820.
(32) Rubinstein, M.; Colby, R. H. *Polymer Physics*; Oxford University Press: New York, 2003.
(33) Cangialosi, D.; Alegría, A.; Colmenero, J. *Phys. Rev. E* **2007**, *75*, 011514.
(34) Lodge, T. P.; McLeish, T. C. B. *Macromolecules* **2000**, *33*, 5278.
(35) Lund, R.; Plaza-Gracía, S.; Alegría, A.; Colmenero, J.; Janoski, J.; Chowdhury, S. R. Quirk, R. P. *Macromolecules*, submitted.
(36) Arbe, A.; Richter, D.; Monkenbusch, M.; Allgeier, J.; Arbe, A.; Colmenero, J.; Farago, B.; Cheol Bae, Y.; Faust, R. *J. Chem. Phys.* **1999**, *111*, 6170.
(37) Logotheti, G. E.; Theoodorou, D. N. *Macromolecules* **2007**, *40*, 2235.
(38) Watanabe, H.; Yamada, H.; Urakawa, O. *Macromolecules* **1995**, *28*, 6443.